CALCULATION OF VORTEX FLOWS ON COMPLEX CONFIGURATIONS

B. Maskew and B.M. Rao
Analytical Methods, Inc.
Redmond, Washington

Abstract

The calculation of aerodynamic characteristics of complex configurations having strongly coupled vortex flows is a non-linear problem requiring iterative solution techniques. This paper discusses the use of a low-order panel method as a means of obtaining practical solutions to such problems. The panel method is based on piecewise constant source and doublet quadrilateral panels and uses the internal Dirichlet boundary condition of zero perturbation potential. The problems of predicting vortex/surface interaction and vortex separation are discussed. Some example calculations are included but further test cases have yet to be carried out, in particular for comparisons with experimental data. The problem of convergence on the iterative calculation for the shape of the free vortex sheet is addressed and a preprocessor routine, based on an unsteady, two-dimensional version of the panel method, is put forward as a cost-effective way of generating an initial vortex structure for use as a starting solution for general configurations.

Introduction

The vortex flows generated on highly swept edges and slender body parts of flight vehicles at high angles of attack are a constant topic for research (e.g., Refs. 1 and 2). The objectives are not only to understand the vortical flow separations, but also to exploit them in designed, structurally stable flow patterns that enhance vehicle performance and extend the range of angle of attack for controlled flight. The complex situation of viscous separation, vortex generation and vortex interaction with downstream parts of a configuration poses a difficult non-linear problem for any attempt at calculating the aerodynamic characteristics of these flows. However, if the location of vortex separation is well defined--such as along sharp edges, strakes, etc.--then practical solutions can be obtained using inviscid methods (e.g., see the review by Smith[1]). Vortex separation from rounded edges requires viscous effects to be included in the computation, but because the viscous regions are largely confined to thin boundary layers, thin helical vortex sheets and small vortex cores, in many cases boundary layer/potential flow iterative approach offers a practical alternative to a full Navier-Stokes analysis. Treatment of vorticity decay and vortex bursting may require a more sophisticated approach, e.g., embedded zonal modelling using a local Navier-Stokes calculation, but again, simple modelling even on a semi-empirical basis, may provide a practical alternative for engineering calculations.

This paper discusses the use of a surface singularity panel method as a practical means of calculating subsonic aerodynamic characteristics of complex configurations with extensive vortex flows and strong vortex/surface interaction. Earlier methods applied to this problem were based mainly on conical flow assumptions (see reviews by Smith[1] and Peake and Tobak[2]) and were therefore restricted to slender planforms. Later, vortex-lattice calculations (see Vortex-Lattice Workshop[3]) provided loading distributions for a wider range of planform shapes, but details of surface pressures were not included. More recently, a high-order panel method[4] has been applied to leading-edge vortex calculations using an iterative procedure to determine the shape of the feeding sheet and location of the vortex core. In principle, such a method should be applicable to very general configurations; however, so far, applications beyond the conical flow conditions have shown poor convergence characteristics resulting in excessive computation times.

The present method, program VSAERO (for Vortex Separation AEROdynamics), is based on piecewise constant source and doublet singularity panels representing the vehicle surface and the Dirichlet boundary condition of zero perturbation potential is applied at an internal control point on each panel. The method, which has been applied to a number of complete aircraft configurations, gives comparable accuracy[5] to higher-order methods at a considerably lower computing cost. This makes it an attractive basis for treating non-linear problems requiring iterative procedures, e.g., vortex/surface interaction, relaxed wake and viscous/potential flow calculations, and also unsteady problems requiring a time-stepping approach.[6] Further, the simple basis of this panel method lends itself to easier treatment of general problems with extensive separation from arbitrary lines.[7]

In the treatment of vortex separation, the vortex cores, thin feeding vortex sheets and wakes are modelled using doublet panels. Most of the present discussion concerns the case with prescribed separation lines. The inviscid calculation with prescribed separation line is likely to be of use by itself in many instances: if vortex flows are to be exploited in a constructive manner in order to enhance vehicle performance and handling, then it is important that stable flow patterns with controlled separation lines be obtained by design and that unstable, moving separation lines be eliminated if possible. Stable flow patterns of vortex separation have already been identified and classified (e.g., Ref. 2) for a number of situations using topological arguments and also experimental observation.

The inviscid calculation with prescribed separation line is also a necessary step during method development to establish a numerically stable procedure for the more general "rounded edge" case before allowing completely "hands-off" calculations with the fully coupled method. The latter involves relaxed wake iterations and potential flow/boundary layer iteration analyses in which the location of separation lines is part of the solution. This

application is discussed briefly in the paper.

In the iterative calculation for the shape of the separated vortex system, convergence to a unique solution is still a problem for the more general cases. It is helpful to start the calculations with an initial vortex structure that has a close approximation to the right shape. For example, analyses of leading-edge vortices on simple delta wings can be started using a conical flow solution. More complex configurations, however, do not usually have such a clear cut starting solution. The present paper includes a description of a method that has been developed to generate initial vortex structures on more general configurations. This method, which is being coupled with the VSAERO code, is based on the unsteady cross-flow analogy of steady three-dimensional flows and is essentially a two-dimensional version of the VSAERO panel model. The method is used to generate solutions in a series of cross-flow planes proceeding in the streamwise direction along the configuration. The approach is similar to that used by Marshall and Deffenbaugh[8] for a circular body except that in the present case use of the panel method allows arbitrary section shapes to be treated in each cross-flow plane. Also, the location of vortex separation must be input to the code at this time. The calculated growth of the vortex system with time (i.e., with distance downstream) describes the three-dimensional shape of the vortex structure which can then be used as a starting solution for the three-dimensional calculations.

Vortex/Surface Interaction

Two-Dimensional Investigation

One of the main factors influencing the success of aerodynamic calculations on configurations with vortex flows is the ability to calculate pressures in the strong interaction zone of a close vortex/surface encounter. Panel methods, even with high-order formulations, often have difficulties in such situations. The basic problems associated with this calculation were investigated[9] for the case of an infinite potential vortex in the presence of a plane. It was concluded that the main factor affecting the accuracy of the surface velocity prediction is the panel density; i.e., the density of control points where the boundary conditions are enforced; the order of the singularity model has only a minor influence. Thus, use of higher panel densities in the regions where vortices are expected to occur is one way of improving predictions of vortex/surface interaction and, in such a treatment, low-order panels are likely to be more cost-effective than high-order panels (unless the high-order formulation was based on the local form of the interference). In any event, the distance between control points should generally be less than the local height of the vortex above the surface.

Subpanel Technique

Another way of improving the vortex/surface interaction calculation has been evaluated.[9] This is a technique based on a subpanel model coupled with an applied doublet distribution. The latter is essentially an initial approximate solution and is related locally to the form of the vortex-induced surface doublet distribution in the vicinity of the vortex.[9] Thus, when evaluating a panel's influence at a point close by, the panel is divided into a number of subpanels. Each subpanel has a uniform singularity distribution, but the singularity value at each subpanel center is obtained partly by second-order interpolation through panel center (unknown) values and partly from the local applied doublet value. Thus, each panel's subpanel system provides a more detailed description of the local singularity distribution and also the surface geometry, Figure 1.

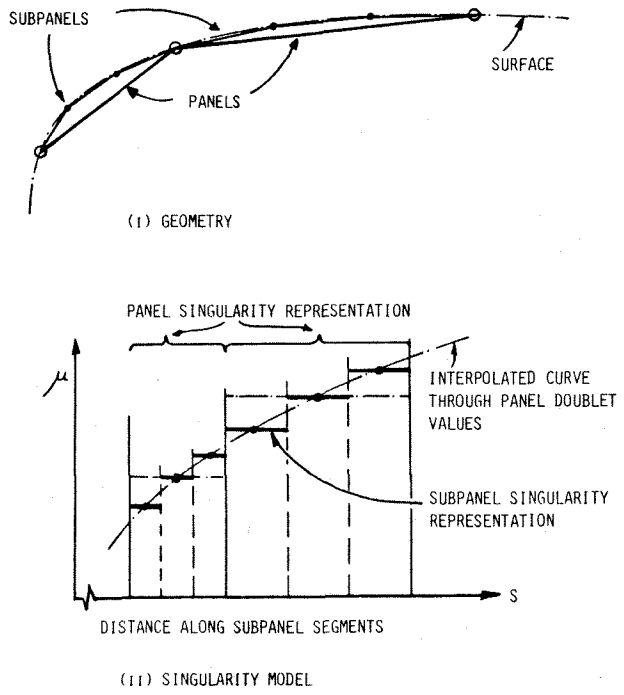

Fig. 1. Subpanel Model (3 Subpanels per Panel Shown).

When an applied doublet distribution having the approximate form of the solution is placed on the subpanel model, part of the influence expression can be evaluated directly and combined with the onset flow; the solution of the boundary condition equations then provides a correction singularity distribution which, when combined with the applied part, satisfies the boundary condition specified at the panel control points. In iterative and time-stepping calculations the above procedure can be used to advantange in that each successive doublet solution can be combined with the applied doublet distribution for use in the next cycle. In this way, each solution is looking for a perturbation over the previous solution.

The subpanel representation of a panel is only accessed when evaluating the panel's influence within a certain distance from the panel center. This "near-field" distance is normally about three times the panel width. The extra computation required for the subpanel technique, therefore, is not significantly greater than for the basic panel method.

Vortex/Airfoil Section

Application of the technique is demonstrated in Figure 2 for the case of a CLARK-Y airfoil section in the presence of a vortex and sink. V.J. Rossow of NASA Ames provided an exact solution for this case using a transformation technique.[10] The calculations are in excellent agreement with the exact solution for both the streamlines (Figure 2(a)) and for the surface pressure distribution, Figure 2(b). Details of the top of the suction peak, which is associated with a reversed flow

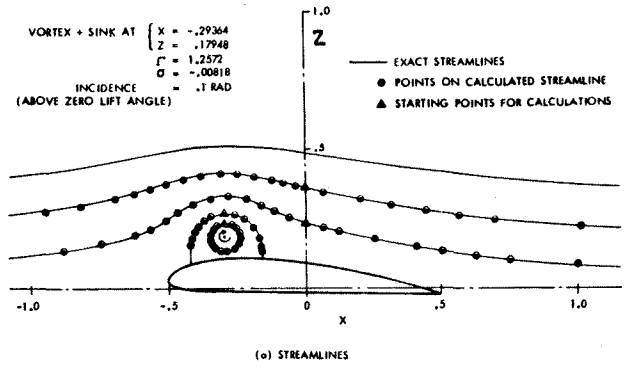

(a) STREAMLINES

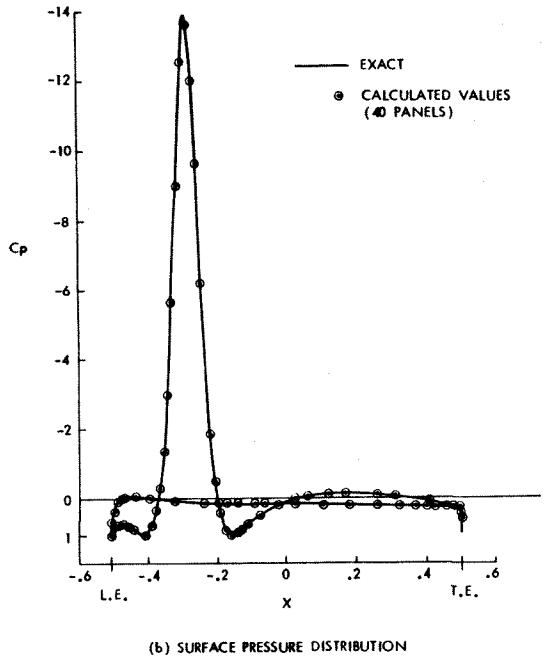

(b) SURFACE PRESSURE DISTRIBUTION

Fig. 2. Comparison of Calculated and Exact Solutions for a CLARK-Y Airfoil in Presence of a Vortex and Sink.

direction, are shown in Figure 2(c) for various subpanel densities; viz., 0, 3, 5 and 7 subpanels per panel. The basic solution with 40 panels (no subpanels) has a significant error in the peak suction value; also, the location of the peak is offset. Notice, however, that there is only one control point station in the interval plotted. For the basic panel model (without subpanel) the applied doublet distribution has no way of "improving" the onset flow conditions at the panel control points. With three subpanels per panel, however, there is a significant improvement in accuracy, not only in the value but also in the location of the peak. Additional but less significant improve-

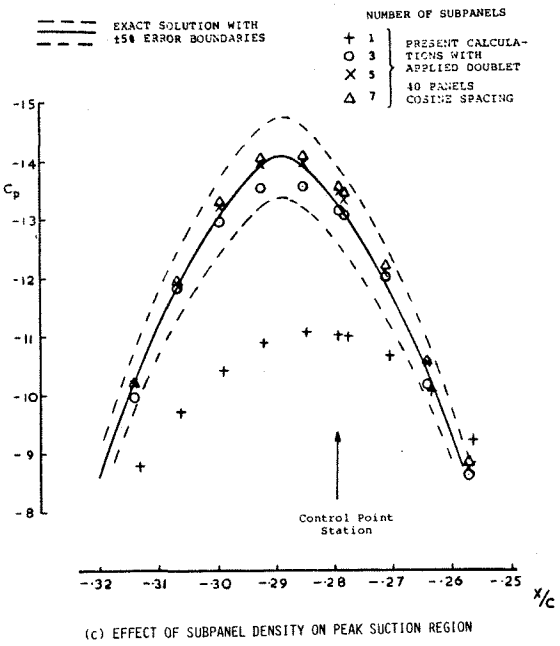

(c) EFFECT OF SUBPANEL DENSITY ON PEAK SUCTION REGION

Fig. 2. Concluded.

ments are indicated for higher subpanel densities. (The "converged" solution appears to have a small over-prediction in C_p; however, there is a possibility that the circulation value for the "exact" case might not have settled down completely in the transformation iteration.)

Vortex/Wing Encounter

The surface singularity code, VSAERO, for the three-dimensional case,[5] has been applied to a number of configurations with strong vortex interaction. Several exploratory calculations have been performed on the basic problem of a wing in the presence of an oncoming vortex wake. Various interacting situations have been examined. One case in which the wake from an upstream vertical surface actually intersects the horizontal downstream wing is discussed in a reserve paper by Clark and Maskew for the present proceedings. (That paper also includes practical applications of the code to complete configurations.) Another case is discussed here in which a tip vortex from the upstream surface passes close to the upper surface of the downstream wing. A general view of the configuration and vortex wake is shown in Figure 3(a) after three wake shape iterations and one viscous/potential iteration. The oncoming vortex system--which passes over the downstream wing at about mid-semispan--is generated by a vertical flat plate set at 20° (horizontal) angle of attack. The plate has an aspect ratio of 2.0 and a chord of .5. The tip edges are raked back at 5°. The horizontal wing has an aspect ratio of 4.0, a chord of 1.0 and a NACA 0012 section. The wing leading edge is placed at one wing chord length downstream of the plate trailing edge. The vertical plate is represented by a 3 x 12 panel array; the wing has a 24 x 20 array of panels on the main wing surface and a 3 x 12 array on the half-round tip. The complete configuration shown in Figure 3 was run with a vertical

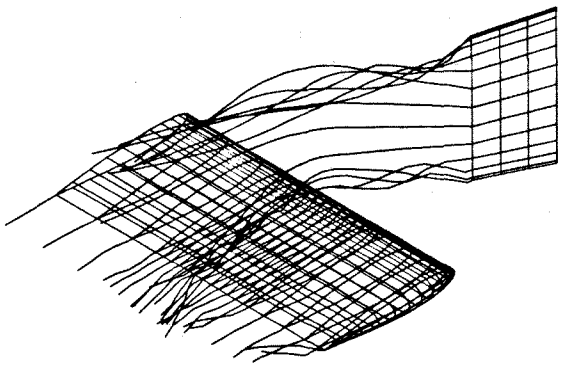

(a) General View

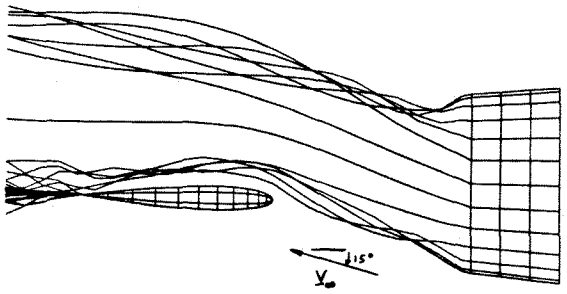

(b) Side View

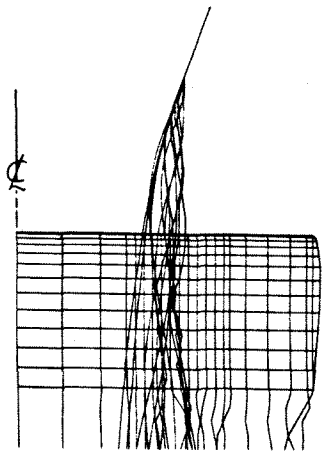

(c) Top View

Fig. 3. Calculations of a Vortex/Wing Encounter.

plane of symmetry at y = 0 and a (vertical) angle of attack of 15°.

The side view of the configuration (Figure 3(b)) after the wake shape calculations shows different rollup characteristics on the two tip vortices from the plate, which is affectively at 15° of "yaw" due to the general onset flow. The lower vortex roll-up and trajectory are clearly influenced by the presence of the wing. the general view, Figure 3(a), and the top view, Figure 3(c), show evidence of a secondary vortex roll-up in the wing wake occurring just outboard of the oncoming vortex location. This secondary vortex contains

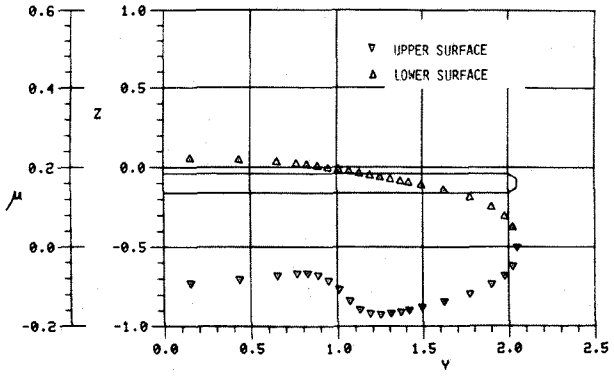

(d) Spanwise Cut through the Doublet Distribution at x/c = .25

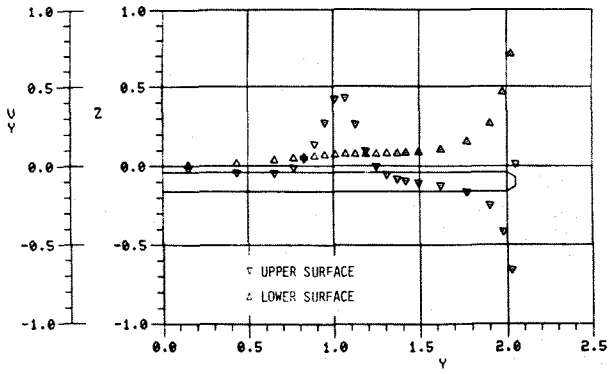

x/c = .25

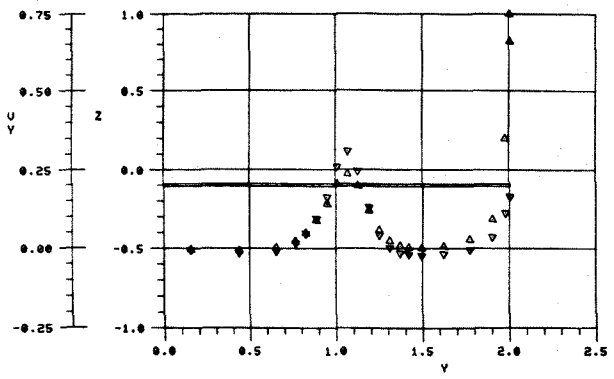

x/c = .004

(e) Spanwise Cuts through the Vy Distribution at x/c = .25 and .004

Fig. 3. Continued.

"negative" circulation induced on the wing by the oncoming vortex. The build-up towards this secondary shedding is very evident in spanwise cuts through the surface doublet (i.e., velocity potential) distribution; e.g., Figure 3(d) shows a cut at x/c = .25. The effect is clearly predominant on the upper surface where we can see the reversed doublet gradient in the vicinity of the passing vortex: the lower-surface doublet distribution has negligible local disturbance due to the vortex. It is encouraging to see such remarkably good

behavior of the doublet solution especially in the vicinity of the vortex and also around the tip edge where the panelling was left very sparse.

The spanwise distribution of Vy, derived from the doublet distribution in Figure 3(d), is given in Figure 3(e) for the station x/c = .25. The positive peak in Vy on the upper surface at y = 1.05 stands out in contrast to the almost monotonic behavior of the lower surface Vy distribution. The latter gradually builds up in the positive spanwise sense, finally speeding up to go around the tip edge then back again (negative) on the outboard upper surface. This characteristic shows a marked rapid change in comparison with the Vy spanwise distribution near the leading edge at x/c = .004, Figure 3(e). At this station the oncoming vortex induces essentially the same (positive) spanwise flow on both upper and lower lines. Also, the differential flow pattern between upper and lower surfaces around the tip edge has not had a chance to develop at this station. The corresponding spanwise cut through the pressure distribution, Figure 3(f) shows the characteristic "upwash/downwash" effect on either side of the initial vortex encounter: this increases the suction peak on one side and suppresses it on the other. This interaction is accompanied by a differential movement of the stagnation line (or attachment line) on the lower surface as we pass through the vortex location. Further downstream the disturbance in the pressure distribution is primarily related to the positive peak in Vy on the upper surface (Figure 3(e) for x/c = .25). The presence of this positive Vy region in what would have been a monotonic negative Vy distribution in the absence of the vortex causes two points of zero Vy to occur at stations y = 1.3 and .72. The latter is a point near a line of streamline divergence; i.e., an attachment line associated with flow coming over the top of the vortex, impinging on the wing and dividing to go either inboard, or outboard back under the vortex. The outboard zero Vy station is a point near a line of streamline convergence; i.e., a line of flow departure from the surface. It is interesting to observe that this station essentially coincides with the location of the secondary vortex observed in Figure 3.

The convergent/divergent characteristics of the local streamlines is confirmed in Figure 3(g). This shows the path of several calculated (external) upper surface streamlines in the vicinity of the vortex. Boundary layer calculations (see later) performed along these streamlines indicate a zone of separation towards the wing trailing edge and just outboard of the vortex track.

Finally, a vertical cut through the field velocities calculated just behind the wing trailing edge at station x/c = 1.3 (Figure 3(h)) shows the strong interacting vortex flows of this configuration. The wing tip vortex and the velocity shear associated with the wing wake are very evident on the right of the figure. Comparing the locations of the two vortices from the vertical, upstream plate, the lower vortex has clearly tracked outboard due to its encounter with the wing. The flow field survey was taken between spanwise stations y = .3 to 2.4 (the wing semispan is 2.0).

The entire calculation described above took 430 CP seconds on a Cyber 176 computer. It involved

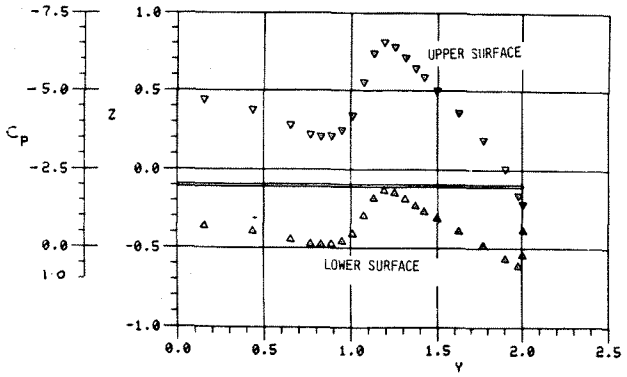

(f) Spanwise Cut through the Pressure Distribution at x/c = .004

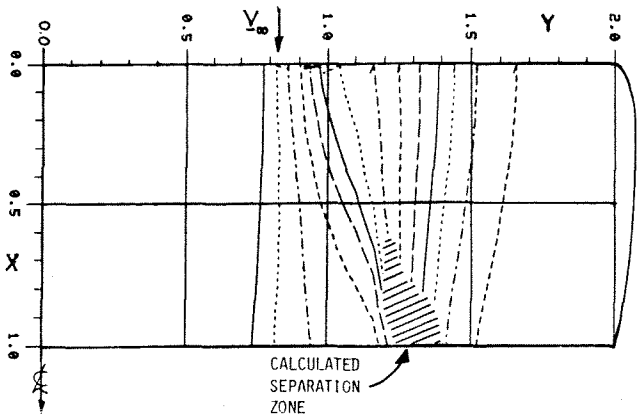

(g) Streamlines (External) Calculated on Wing Upper Surface

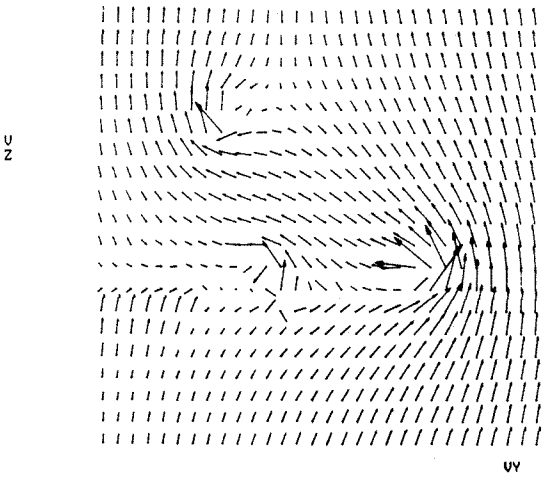

(h) Velocity Survey in Cross-Flow Plane at x/c = 1.3

Fig. 3. Concluded.

550 surface panels and 400 wake panels on one side of the assumed vertical plane of symmetry. Three wake shape iterations were performed with one viscous/potential iteration (i.e., a total of 4 potential flow solutions for surface velocity and pressures). Sixteen surface streamlines were calculated for the boundary layer analysis, and finally 600 off-body points were analysed in the cross-flow velocity survey.

The main purpose of the above calculation was to explore the behavior of the program applied to this type of problem. Following the encouraging results obtained in this and other similar calculations, it is now intended to perform correlations with experimental data including the influence of viscous vortices. So far, suitable data with good surface pressure measurements, flow visualization on the surface and flow field, and flow-field velocity measurements, has proven difficult to find. Vortex meander in the wind tunnel often hinders the measurement of good data.

Initial Vortex Structure

One of the basic problems of the iterative calculation procedure for general vortex separations is that unless a reasonable guess can be made for the initial vortex structure, the calculations can take a long time to converge or they may even diverge. A good initial vortex structure is, therefore, crucial for practical calculations. Structures based on conical flow solutions have been used in the past,[4] but are not good enough for the general case. To overcome this problem an extension of the two-dimensional code, discussed above for basic vortex/surface interaction calculations, has been investigated for generating initial vortex structures[11] based on the unsteady cross-flow analogy of three-dimensional steady flows. The objective is to use the initial vortex structure as the starting solution for the three-dimensional program, thereby reducing the number of vortex-wake shape iterations required in the main code and possibly reducing the chance of a divergent solution.

The two-dimensional code is applied in a time-stepping calculation on a series of cross-flow sections through the configuration, Figure 4. Consider one of these sections, Figure 5. The section surface is represented by a set of flat panels (each of which may be divided into an odd number of subpanels as discussed earlier). Each surface

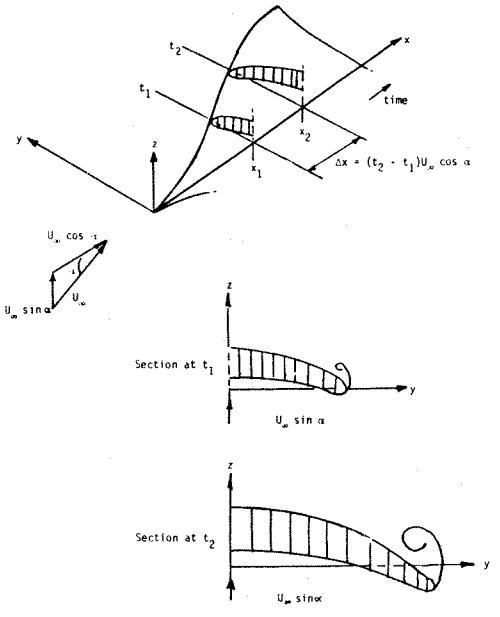

Fig. 4. Unsteady Cross-Flow Analogy.

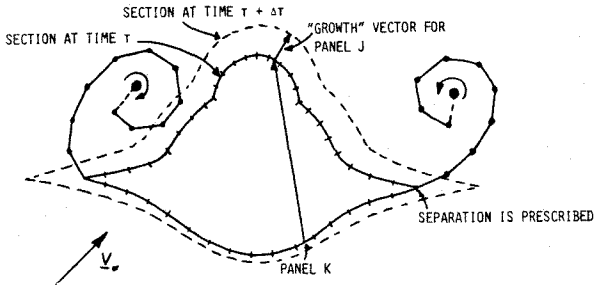

Fig. 5. Sections in the Cross-Flow Planes.

panel has a uniform distribution of source and doublet singularities. The locations of vortex separation are supplied in the program input at this time. The free vortex sheets are represented by doublet panels.

Boundary Conditions

The internal Dirichlet boundary condition of zero perturbation potential is satisfied at the center of each surface panel. This boundary condition was used earlier by Johnson and Rubbert[12] and by Bristow and Grose,[13] but in high-order formulations. The piecewise constant singularity model briefly described here has the same basic equation given earlier by Morino and Chen,[14] who used a direct application of Green's Theorem in the external flow field. Several test cases[5] have demonstrated that--in subsonic flow at least--with similar panel densities the low-order method gives equivalent accuracy to the high-order solutions.

The equation to be satisfied at each surface panel control point has the form:[5]

$$\sum_{\substack{K=1\\K=J}}^{N_S} \left\{\mu_K\, C_{JK}\right\} - 2\pi\mu_J + \sum_{K=1}^{N_W} \left\{\mu_{W_K}\, C_{JK}\right\} + \sum_{K=1}^{N_S} \left\{\sigma_K\, B_{JK}\right\} = 0; \qquad J=1,\, N_S \tag{1}$$

where N_S, N_W, are the total number of panels on the body surface(s) and free vortex wake(s), respectively. B_{JK}, C_{JK}, are the perturbation potentials at the J^{th} control point due to unit uniform source and doublet distributions, respectively, on panel K. The basic unknowns in the equation are the surface panel doublet values, μ_K, K=1, N_S.

The surface panel source values, σ_K, K=1, N_S, are determined by the external Neumann boundary condition and can be evaluated at each step[6] in the time-stepping calculation:

$$\sigma = V_N + \underline{n} \cdot \underline{V}_S - \underline{n} \cdot \underline{V}_\infty \tag{2}$$

where $\underline{n}$ is the local outward unit normal vector; V_N is the resultant normal velocity component used to represent boundary layer displacement effect by

transpiration and also inflow/outflow for engine inlet/exhaust representation; $\underline{V}_S$ is the local transient velocity of the surface due to rotation,[6] translation, growth,[9] etc., and $\underline{V}_\infty$ is the local onset flow in the cross-flow plane. The onset flow can be made non-uniform using an initial three-dimensional solution. In this way three-dimensional effects such as Kutta condition, wake and other interference effects can be approximately represented in the cross-flow plane solutions.

[Note that in the present application Eq. (1) should strictly include a contribution from the surface at infinity due to the net source value represented by the terms $V_N + \underline{n} \cdot \underline{V}_S$ in Eq. (2). The term would affect the pressure coefficient (in the $\partial\phi/\partial t$ term) but would not affect the field velocities which are of main interest here.]

The body "growth" term in $\underline{V}_S$ is evaluated by comparing the present cross-flow section with the next one, Figure 5. The "movement" of a corresponding surface point from one plane to the next is divided by the time increment representing the axial movement. This time interval, Δt is evaluated as:

$$\Delta t = \frac{\Delta x}{U_x} \tag{3}$$

where U_x is the x-component of the general onset velocity for the complete configuration and Δx is the distance between the two cross-flow planes.

The solution of Eq. (1) gives the surface doublet values. A similar equation--but with velocity influence coefficients rather than velocity potential coefficients--is then applied to calculate velocities at points on the free vortex sheets.

Vortex Model

The free vortex sheet leading to the vortex core is modelled by a set of doublet panels, Figure 6. The doublet value associated with a point in the sheet is essentially constant with time. The location of each point is calculated in the time-stepping procedure moving from one plane to the next (Figure 6) by convecting it along the local calculated velocity vector. During this process, a new piece of vortex sheet is formed from the separation point (Figure 6). The length of the new segment is

$$S_1 = \Delta t \; V^t_{sep}$$

where V^t_{sep} is the modulus of the resultant velocity at the separation point. The new doublet strength at the separation point at time, $t + \Delta t$, is

$$\mu_1^{t+\Delta t} = \mu_1^t + S_1(\gamma_U + \gamma_L) \tag{4}$$

where $\mu_1 = \mu_U - \mu_L$ is the jump in doublet value across the vortex sheet as it leaves the surface (Figure 6).

Equation (4) essentially satisfies the unsteady condition relating the change in circulation on the wing (μ_1) to the amount of circulation shed into the wake in the interval Δt. It is assumed that the shedding occurs at constant vorticity, γ_U, γ_L, respectively on the upper and lower surfaces at the separation point. (The doublet and vorticity values at the separation point are extrapolated from panel center values on each side of the point.)

Two schemes are employed to help stabilize the vortex tracking over the large time required to traverse a complete configuration and also to control the number of wake panels. The first scheme is a vortex amalgamation procedure[9] similar to that used by Moore.[15] The procedure is controlled by the rotation angle, θ, measured from a line drawn from the vortex core to the separation point. When a point on the free sheet has moved around the core by more than a specified amount, θ_{merge}, that part of the sheet is merged with the core which is then relocated at the centroid of the combined circulation. This scheme avoids having to follow a large number of turns of the free sheet. It has been observed, however, that at least 1½ turns should be represented when the surface pressure distribution under the vortex is required.[9] This spreads the "base" of the suction region under the vortex, whereas a single amalgamated vortex core has a much narrower base and a higher peak suction value.

The second stabilizing scheme incorporated in the program is a vortex redistribution procedure similar to that used by Fink and Soh[16] and by Sarpkaya and Shoaff.[17] Linear interpolation was employed in this redistribution procedure rather than using a higher-order interpolation scheme such as described recently by Bromilow and Clements.[18] However, the latter is being considered for application in the early part of the vortex sheet attached to the separation point.

The free-sheet panels and the doublet values are redistributed after each time step in such a way that the points are uniformly spaced along the free sheet. The scheme allows the number (and, hence, size) of free-sheet panels to be controlled independently of time-step size.

The free-sheet vortex model has proven very successful in a number of test cases,[9],[11] and the two-dimensional code is now being assembled as a preprocessor code to be run with the VSAERO program.

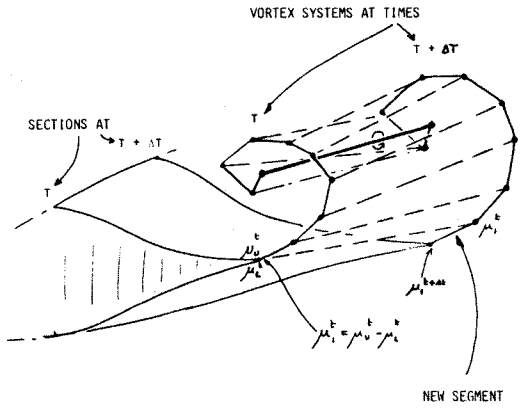

Fig. 6. Vortex Sheet Model.

Example Calculations

Thin Delta Wing

The preprocessor code was applied to the delta wing investigated experimentally by Hummel.[19] This has a 76° leading-edge sweep angle and the 20° incidence case was considered. Twenty panels with three subpanels per panel were used on each section. The calculations were started at x/c = .1 (t = 0). the computed vortex core positions and the experimental suction peak locations[19] are compared in Figure 7 and show good visual agreement. The slight "wobble" in the computed vortex core position is due partly to the merging procedure and partly because of the core rotation about the centroid of shed vorticity. The calculations used θ_{merge} angle of 180° and were carried out for 140 time planes. The total calculation took 320 CP seconds on a Cyber 175, which makes it a very cost-effective procedure for generating a starting solution. Although the above calculation was for a simple planform with a triangular section, the procedure is applicable to general planform and section shapes. In principle, wing-bodies with multiple separations can also be treated.

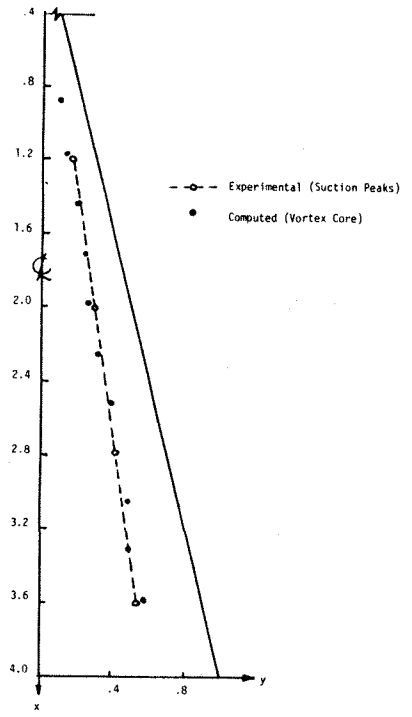

Fig. 7. Comparison between Chordwise Experimental Suction Peaks and Computed Vortex Core Locations on a Thin Delta Wing.

Ogee Wing

A series of vortex sheet shapes calculated on an ogee wing at 21° angle of attack is shown in Figure 8. The calculation started at x/c_R = .1 and a total of 90 time planes were calculated. It is interesting to observe the changes in the initial shape of the sheet as it leaves the surface at various stations; i.e., the influence of the leading-edge sweep on rate of growth in the two-dimensional calculation. Also, the ellipticity in the

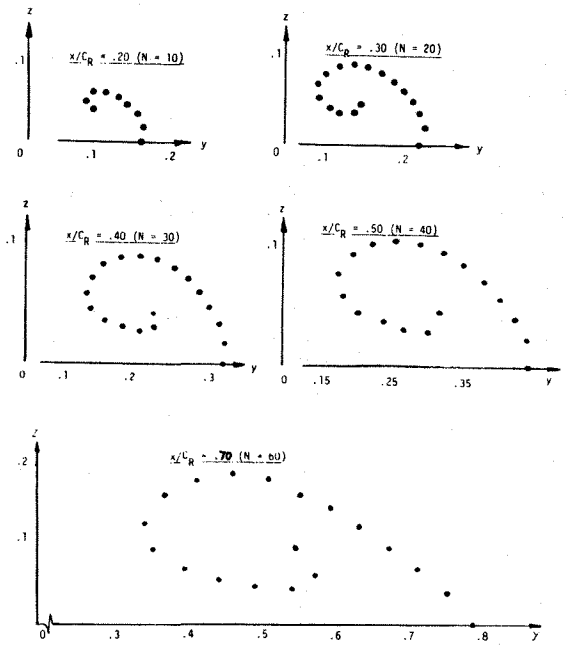

Fig. 8. Calculated Vortex Structure on an Ogee Planform.

shape of the sheet is very pronounced in the region of smallest sweep (maximum growth rate). The amalgamation angle was set at 360° for these calculations in order to represent the first passage of the free sheet over the surface. A second run was conducted with a θ_{merge} angle of 180°.

Figure 9 compares the calculated vortex sheet shape at x/CR = .6 with the starting and converged solutions calculated at NASA Langley using the NASA Langley/Boeing free vortex-sheet code (described in Ref. 4). Allowing for the difference in the vortex merging angles, the present solution would clearly provide an improved starting solution for the three-dimensional code.

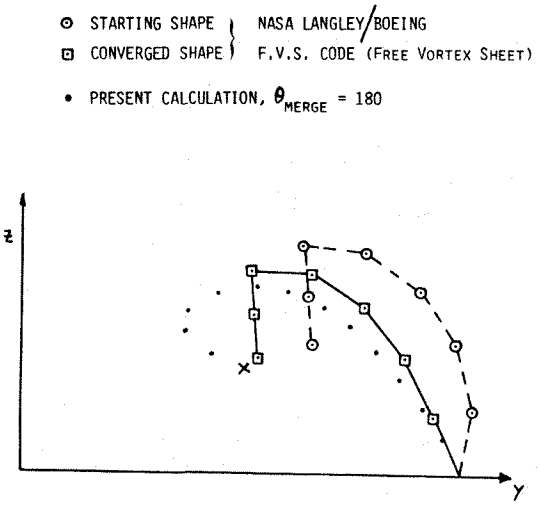

Fig. 9. Comparison of Calculated Vortex Sheet Shapes at X/CR = .6 on Ogee Wing.

A planform view is given in Figure 10, which compares the amalgamated vortex trajectory (not the vorticity centroid) with the surface flow features from experiment.[20] The path lies somewhat ahead of the line indicated by experiment, but this may be due to the absence of the secondary vortex in the calculation. In principle, a secondary vortex--with prescribed separation line--can be modelled in the calculation but this has not been tried yet. The trailing-edge Kutta condition was not represented in this calculation (e.g., by using a non-uniform onset flow). This omission has not seriously affected the vortex trajectory except over the very last part of its path over the wing.

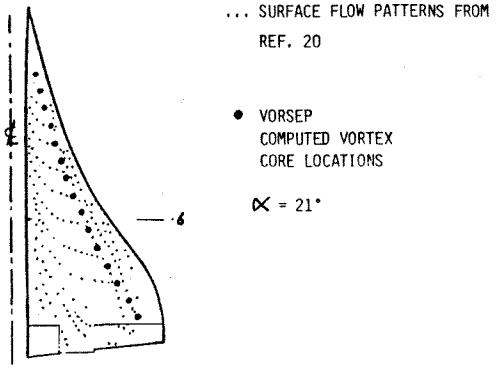

Fig. 10. Comparison of Computed Vortex Core Locations with Experimental Surface Flow Patterns on Ogee Wing.

Bent Rectangular Wing

The program was applied to a rectangular wing of aspect ratio 1/4 and with a 20° mid-chord bend to test a strong camber effect on edge vortex formation. This model, which Wickens tested earlier,[21] is set at 20° incidence giving a 40° angle of attack to the flow on the rear portion. The experimental observations[21] clearly show a double vortex system--one from the leading edge, the other from the kink. The calculation started at x/c = 0.1 and 81 time planes were used. Vortex structures are shown in Figure 11 at three stations. Although a definite bulge has appeared in the free sheet, the detailed roll-up of the second vortex has been smeared out by the redistribution scheme. A higher density of wake panels would improve the definition of the local roll-up. Even so, the bulge does migrate around the main vortex (Figures 11(b) and 11(c)) in a similar way to the experimentally observed second vortex (see inset from Figure 5 of Ref. 21). An intermediate amalgamation scheme covering the second vortex would improve the numerical behavior of the calculation.

Location of Separation Lines

On general configurations the location of the separation lines is not always known beforehand. Some coupling has been made between the VSAERO panel code and integral boundary layer codes. Following a solution of the surface doublet distribution, a family of (external) surface streamlines is calculated; e.g., Figure 12. Boundary layer calculations are then performed along each

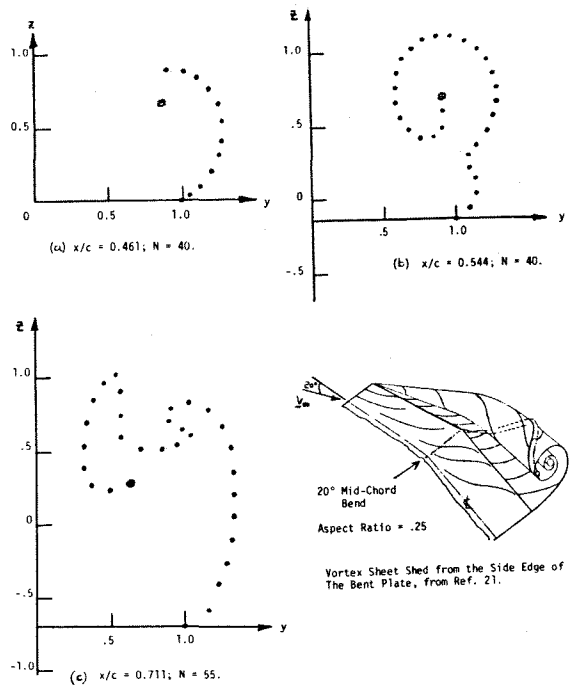

Fig. 11. Calculated Vortex Sheet Shape at Three Vertical Sections on a Bent Plate at 20° Incidence.

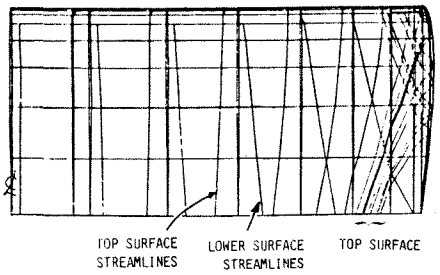

Fig. 12. Streamlines (External) Calculated on a Rectangular Wing with NACA 0012 Section.

streamline. The boundary layer codes, which are described in Ref. 22, are based on locally axisymmetric conditions with surface curvature and streamline convergence/divergence effects included.

Calculations were performed on the rectangular wing of aspect ratio 4. The wing section is NACA 0012. Angles of attack of 4°, 8°, 12° and 16° were analysed. In each case, a family of surface streamlines (e.g. as shown in Figure 12) was calculated. Separation points calculated by the boundary layer routine were then superimposed on the calculated streamlines to indicate the locus of separation. Figure 13 shows the extent of tip-edge separation as a function of angle of attack and two Reynolds numbers. The results represent the conditions for the first viscous/potential flow iteration cycle; i.e., before modelling the tip-edge vortex as described in Reference 6.

Figure 14 shows the plan view of the calculated separation boundaries for a range of angles of

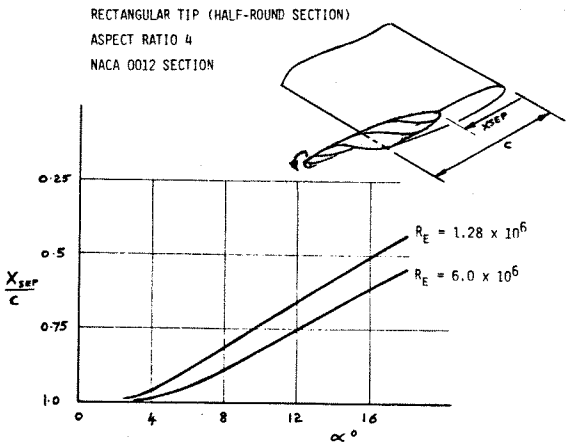

Fig. 13. Effect of Angle of Attack on Extent of Tip-Edge Separation.

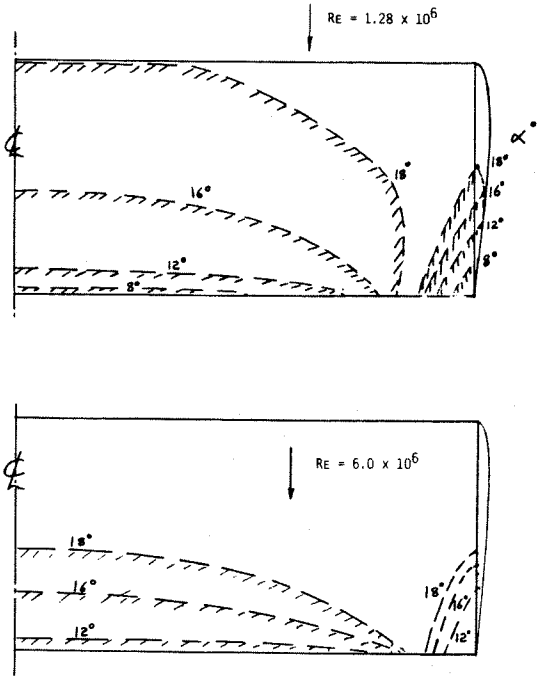

Fig. 14. Calculated Separation Boundaries on a Rectangular Wing for a Range of Incidence and Two Reynolds Numbers.

attack. In addition to the tip-edge separation, the separation boundaries over the inner part of the wing are also included. Figure 14(a) shows the boundaries for a Reynolds number of 1.28 x 10^6 and Figure 14(b) is for a Reynolds number of 6.0 x 10^6. At the lower Reynolds number, some laminar separation with no reattachment is indicated at 18° in the inboard region. At the higher Reynolds number, the extent of separation is considerably lower. It should be emphasized that the calculated separation boundaries in Figure 14 are for the initial solution only and would be expected to change when the separated vortex sheets are modelled in the analysis.

It is interesting to compare the shape of these calculated separation boundaries with experimental observations. Figure 15 taken from Ref. 23

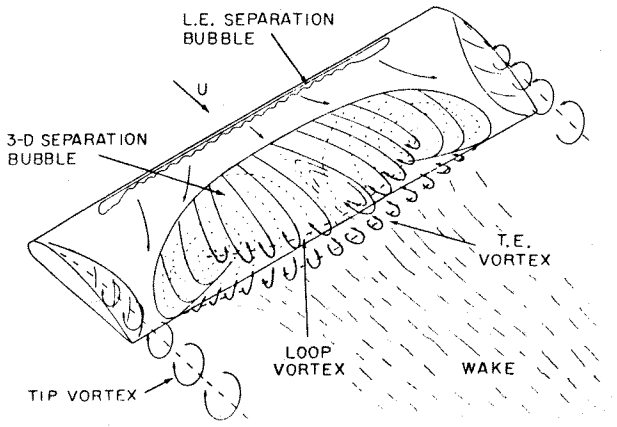

Fig. 15. Sketch of Flow Field on a Wing Just Beyond the Stall--From Ref. 23.

is a sketch of the separated flow field of a rectangular wing. The calculated and experimental separation patterns are in remarkably close qualitative agreement.

An interesting feature of the separation boundaries (Figure 14) is that the inboard and tip-edge separations form two distinct zones even before the separated vortex sheets are modelled. A family of streamlines proceeding from the attachment line near the tip leading edge proceed over the upper surface and reach the trailing-edge without separating and form a distinct attached flow zone between the inboard and tip-edge separation.

In Figure 16 three of these "attached" streamlines have been examined and show distinctly different characteristics. Streamline "A" starting

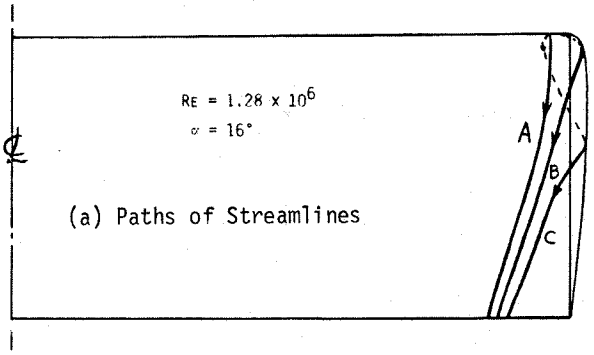

Fig. 16. Three Calculated Streamlines near Tip of Rectangular Wing.

just inboard of the tip on the lower surface proceeds forward around the leading edge and then inboard over the upper surface. Streamline "B" starts at a point just outboard of "A" but "sneaks" around the tip edge onto the upper surface. Streamline "C" is predominantly a lower-surface streamline starting near "A"; however, it eventually passes around the tip edge and then proceeds over the upper surface to the trailing edge. The C_p history is plotted as a function of distance along the streamlines in Figure 16(b). Streamline "A" suffers a high suction peak during its passage over the leading edge and then negotiates a strong adverse pressure gradient over the upper surface.

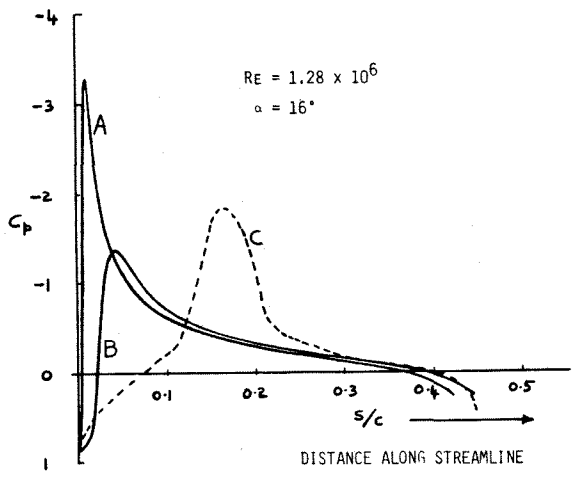

(b) Pressures along Streamlines

Fig. 16. Concluded.

Streamline "B" passes through a mild suction peak on the tip edge and only a moderate adverse pressure gradient on the upper surface. Streamline "C" has a long favorable pressure gradient until it has passed around the tip edge.

Streamlines inboard of "A" have to negotiate higher leading-edge suction peaks and eventually define the inboard separation zone. Streamlines outboard of "C" see their suction peak occurring later along their length, but the peak value rises sharply at stations nearer the trailing edge and this leads to the tip-edge separation zone.

Clearly, the patterns of separation boundaries is very dependent on the section and planform shapes and also on the tip-edge profile. The latter, in particular, strongly influences the tip-edge separation and, hence, the formation of the tip-edge vortex. The VSAERO program is now capable of locating separation boundaries on any tip-edge shape (planform or section profile) and could clearly be applied to a more fundamental investigation of tip-edge vortex formation. Knowledge of the pressure histories and boundary layer characteristics could be used as a guide to suggest changes in tip geometry to control the edge vortex characteristics.

Conclusions

The surface pressure distribution and flow field in a strong potential vortex/surface interaction can be accurately predicted in the two-dimensional situation using a panel method. Plausible solutions for a vortex/wing encounter have been demonstrated in the three-dimensional case using a low-order panel method, VSAERO, with iteration cycles for wake shape and viscous/potential flow effects. Further calculations are needed for comparison with experimental data. Computation times for such cases are very reasonable.

A Preprocessor routine based on a time-stepping two-dimensional panel code promises to be a useful and cost-effective tool for generating starting solutions for the vortex structure on general configurations. This should reduce the number of iterations required by the three-dimensional code applied to such configurations.

Calculations using the VSAERO panel method coupled with integral boundary layer calculations along calculated (external) streamlines have given encouraging results for locating separation lines for edge vortices and for secondary vortices in the presence of a passing vortex.

Acknowledgements

The authors gratefully acknowledge the following support for work reported in this paper. The basic two-dimensional investigation leading to the technique for setting up the initial vortex structure was funded by NASA Langley under Contracts NAS1-15495 and NAS1-16155. The basic three-dimensional VSAERO panel method was developed under Contract NAS2-8788 from NASA Ames. Extensions of this code for modelling massive separations and unsteady tip-edge separation were funded, respectively, by the Office of Naval Research under Contract N00014-78-C-0128 and by NASA Langley under Contract NAS1-15472.

References

1. Smith, J.H.B., "Inviscid Fluid Models Based on Rolled Up Vortex Sheets for Three-Dimensional Separation at High Reynolds Number", AGARD LS 94, (Three-Dimensional and Unsteady Separation at High Reynolds Numbers), May 1978.

2. Peake, D.J. and Tobak, M., "Three-Dimensional Interactions and Vortical Flows with Emphasis on High Speeds", NASA TM 81169, March 1980.

3. "Vortex-Lattice Utilization", NASA SP-405, May 1976.

4. Johnson, F.T. et al., "An Improved Panel Method for the Solution of Three-Dimensional Leading-Edge Vortex Flows", Vol. I--Theory Document, NASA CR-3278, Vol. II--User's Guide and Programmer's Document, NASA CR-3279, 1980.

5. Maskew, B., "Prediction of Subsonic Aerodynamic Characteristics--A Case for Low-Order Panel Methods", Paper 81-0252, Presented at the AIAA 19th Aerospace Sciences Meeting, St. Louis, MO, January 12-15, 1981.

6. Maskew, B., "Influence of Rotor Blade Tip Shape on Tip Vortex Shedding--An Unsteady Inviscid Analysis", Paper 80-6 in Prodeedings of the 36th Annual Forum of the American Helicopter Society, May 1980.

7. Maskew, B., Rao, B.M. and Dvorak, F.A., "Prediction of Aerodynamic Characteristics for Wings with Extensive Separations", Paper No. 31 in Computation of Viscous-Inviscid Interactions, AGARD-CPP-291, September 1980.

8. Marshall, F.J. and Deffenbaugh, F.D., "Separated Flow over a Body of Revolution", J. Aircraft, Vol. 12, No. 2, pp. 78-85, February 1975.

9. Maskew, B., "Calculation of Two-Dimensional Vortex/Surface Interference using Panel Methods",

9. (Continued) NASA CR-159334, December 1980.

10. Rossow, V.J., "Lift Enhancement by an Externally Trapped Vortex", J. Aircraft, Vol. 15, No. 9, September 1978, pp. 618, 625.

11. Rao, B.M. and Maskew, B., "Flows over Wings with Leading-Edge Vortex Separation", NASA CR-165858, April 1982.

12. Johnson, F.T. and Rubbert, P.E., "A General Panel Method for the Analysis and Design of Arbitrary Configurations in Subsonic Flows", NASA CR-3079, 1980.

13. Bristow, D.R. and Grose, G.G., "Modification of the Douglas Neumann Program to Improve the Efficiency of Predicting Component Interference and High-Lift Characteristics", NASA CR-3020, 1978.

14. Morino, L., Chen, L.-T. and Suci, E.O., "Steady and Oscillatory Subsonic and Supersonic Aerocynamics around Complex Configurations", AIAA J., Vol. 13, No. 3, March 1975.

15. Moore, D.W., "A Numerical Study of the Roll-Up of a Finite Vortex Sheet", J. Fluid Mech., Vol. 63, 1974, p. 225.

16. Fink, P.T. and Soh, W.K., "A New Approach to Roll-up Calculations of Vortex Sheets", Proc. Royal Soc. A., Vol. 362, 1978, p. 195.

17. Sarpkaya, T. and Shoaff, R.L., "An Inviscid Model for Two-Dimensional Vortex Shedding for Transient and Asymptotically Steady Separated Flow over a Cylinder", AIAA J., Vol. 17, 1979, p. 1193.

18. Bromilow, I.G. and Clements, R.R., "Some Techniques for Extending the Application of the Discrete Vortex Method for Flow Simulation", Aero. Quart., Vol. 33, February 1982, pp. 73-89.

19. Hummel, D., "On the Vortex Formation over a Slender Wing at Large Angles of Incidence", High Angle-of-Attack Aerodynamics, AGARD-CP-247, January 1979.

20. Collard, D., "Comportement a Haute Incidence D'un Avion de Transport a Aile a Grand Elancement", High Angle-of-Attack Aerodynamics, AGARD-CP-247, January 1979.

21. Wickens, R.H., "The Vortex Wake and Aerodynamic Load Distribution of Slender Rectangular Wings", Canadian Aeronautics and Space Journal, June 1967, pp. 247-260.

22. Dvorak, F.A., Maskew, B. and Woodward, F.A., "Investigation of Three-Dimensional Flow Separation on Fuselage Configurations", USAAMRDL-TR-77-4, March 1977.

23. Winklemann, A.E., "Flow Field Surveys of Separated Flow on a Rectangular Planform Wing", Paper 81-0255, Presented at the AIAA 19th Aerospace Sciences Meeting at St. Louis, MO, January 12-15, 1981.